International Journal of Radiation Oncology biology • physics

www.redjournal.org

Critical Review

Magnetic Resonance Imaging-Guided Adaptive Radiation Therapy: A "Game Changer" for Prostate Treatment?

Angela U. Pathmanathan, MA,[*,†] Nicholas J. van As, MD,[*,†] Linda G.W. Kerkmeijer, PhD,[‡] John Christodouleas, MD,[§] Colleen A.F. Lawton, MD,[‖] Danny Vesprini, MD,[¶] Uulke A. van der Heide, PhD,[#] Steven J. Frank, MD,[**] Simeon Nill, PhD,[*,†] Uwe Oelfke, PhD,[*,†] Marcel van Herk, PhD,[††,‡‡] X. Allen Li, PhD,[‖] Kathryn Mittauer, PhD,[§§] Mark Ritter, PhD,[§§] Ananya Choudhury, PhD,[††,‡‡] and Alison C. Tree, MD[*,†]

The Institute of Cancer Research, London, United Kingdom; [†]The Royal Marsden National Health Service Foundation Trust, London, United Kingdom; [‡]University Medical Center Utrecht, Utrecht, The Netherlands; [§]Elekta, Inc, Philadelphia, Pennsylvania; [‖]Medical College of Wisconsin, Milwaukee, Wisconsin; [¶]Sunnybrook Health Sciences Centre, University of Toronto, Toronto, Ontario, Canada; [#]Department of Radiation Oncology, The Netherlands Cancer Institute, Amsterdam, The Netherlands; [**]The University of Texas MD Anderson Cancer Center, Houston, Texas; [††]Manchester Cancer Research Centre, University of Manchester, Manchester Academic Health Science Centre, The Christie National Health Service Foundation Trust, Manchester, United Kingdom; [‡‡]National Institute of Health Research, Manchester Biomedical Research Centre, Central Manchester University Hospitals National Health Service Foundation Trust, Manchester Academic Health Science Centre, Manchester, United Kingdom; and [§§]University of Wisconsin School of Medicine and Public Health, Madison, Wisconsin

Received Sep 14, 2017, and in revised form Oct 9, 2017. Accepted for publication Oct 12, 2017.

Reprint requests to: Ananya Choudhury, PhD, The Royal Marsden National Health Service Foundation Trust, Wilmslow Rd, Withington, Manchester M20 4BX, United Kingdom. Tel: (161) 918-7939; E-mail: ananya.choudhury@christie.nhs.uk

A.C. and A.C.T. are joint last authors.

A.T., A.C., U.O., S.N., and A.P. have received research and educational travel support from Elekta. Elekta financially supports the MR-Linac Consortium and all member institutes, including research funding. Elekta supports travel costs for consortium meetings. A.T., A.P., N.V.A., U.O., and S.N. acknowledge the support of National Health Service funding to the National Institute of Health Research Biomedical Research Centre at The Royal Marsden and The Institute of Cancer Research. The views expressed in this paper are those of the authors and not necessarily those of the NHS, the NIHR or the Department of Health. Research at the Institute of Cancer Research is also supported by Cancer Research UK (CRUK) (program grant C33589/A19727).

Conflict of interest: L.K., J.C., C.L., D.V., U.A.H., S.F., S.N., U.O., M.H., A.L., A.C., and A.T. are part of the Elekta MR-Linac Research Consortium, which aims to coordinate international research into the magnetic resonance linear accelerator. Elekta and Philips are members of the MR-Linac Consortium. J.C. is an employee of Elekta. L.K. reports grants from Elekta to University Medical Center Utrecht, outside the submitted work. A.C. and M.V. acknowledge the support of the National Institute of Health Research Manchester Biomedical Research Centre. A.C. has received grants from Cancer Research UK, National Institute for Health Research, and Prostate Cancer UK outside the submitted work. N.V.A. has received grants and personal fees from Accuray outside the submitted work. S.J.F. acknowledges U19 National Institutes of Health/National Cancer Institute grant support, is a consultant/advisor for Varian, has received honoraria from IBA and Hitachi, is a board member of American Board of Radiology and American Brachytherapy Society, is a director of C4 Imaging, and has a patent for MRI markers licensed. A.T. has received honoraria from Janssen, Astellas, and Bayer and research funding from MSD outside the submitted work. K.M. has received honoraria from ViewRay, Inc.

Acknowledgments—Figure 5 was provided courtesy of Maria Schmidt, The Institute of Cancer Research.

Int J Radiation Oncol Biol Phys, Vol. 100, No. 2, pp. 361–373, 2018

https://doi.org/10.1016/j.ijrobp.2017.10.020

Radiation therapy to the prostate involves increasingly sophisticated delivery techniques and changing fractionation schedules. With a low estimated α/β ratio, a larger dose per fraction would be beneficial, with moderate fractionation schedules rapidly becoming a standard of care. The integration of a magnetic resonance imaging (MRI) scanner and linear accelerator allows for accurate soft tissue tracking with the capacity to replan for the anatomy of the day. Extreme hypofractionation schedules become a possibility using the potentially automated steps of autosegmentation, MRI-only workflow, and real-time adaptive planning. The present report reviews the steps involved in hypofractionated adaptive MRI-guided prostate radiation therapy and addresses the challenges for implementation.

Introduction

Prostate radiation therapy (RT) techniques have undergone a metamorphosis during the past 2 decades. We have transitioned from 2-dimensional to 3-dimensional (3D) techniques and, subsequently, to intensity modulated RT, image-guided RT (IGRT), and, more recently, to stereotactic body RT (SBRT). Localization strategies have evolved from external skin markings, to 2-dimensional/megavoltage-based bony localization, to complex techniques allowing localization of the target through implanted fiducial markers, electromagnetic beacons, or 3D/kilovoltage volumetric imaging with soft tissue capabilities of in-room computed tomography (CT) or cone beam CT.

However, another wave of technological refinements is fast approaching, with magnetic resonance imaging (MRI)-guided photon RT, modern particle therapy, and the prospect of ultrafast replanning, enabling treatment paradigms previously thought to be science fiction to become reality.

The improvement in precision delivered by these technical changes has synchronized with a change in our RT fractionation. The CHHiP (conventional or hypofractionated high dose intensity modulated radiotherapy for prostate cancer) trial (1) has shown that 60 Gy in 20 fractions is at least as good as 74 Gy in 37 fractions, which has changed the standard fractionation in many countries from 7.5 weeks to 4 weeks. The PACE (prostate advances in comparative evidence) trial (ClinicalTrials.gov identifier, NCT01584258) is randomizing between a similar 4-week schedule and 5-fraction SBRT. As the α/β ratio of prostate cancer is thought to be low (2-5), hypofractionation should improve the therapeutic ratio.

The purpose of the present review is to describe

1. The future implications of the existing evidence on the optimal fractionation for prostate cancer and, ultimately, whether single-fraction RT is feasible
2. How MRI-guided RT (MRgRT) could change the paradigms in prostate cancer RT
3. A road map to overcoming the obstacles to implementation

Search Strategy and Selection Criteria

Published studies for the present review were identified by conducting a search using PubMed, with the following words: "prostate," "radiotherapy," "radiation therapy," "MRI," "MR," "magnetic resonance image," "adaptive," "MR-guided," "MR-linac," "ViewRay," "autosegmentation," "automatic segmentation," "autocontouring," "pseudo-CT," and "substitute CT." The last PubMed search was performed on August 1, 2017. The search included meeting abstracts and was restricted to reports available in English. Further references were identified by a manual search of the reference list of the included studies. Identified studies were first screened by title and/or abstract, with a further full paper screening to generate the final list of studies relevant to the scope of the present review.

Hypofractionation—How Low Do We Go?

Although the ideal dose and fractionation of RT, allowing for maximum tumor control with acceptable toxicity, is far from certain, hypofractionation is increasingly favored (6-8). The α/β ratio for prostate cancer is estimated to be as low as 1.5 Gy (1, 2, 9, 10), suggesting that moderate hypofractionation can be as effective as standard fractionation for prostate RT. This has now been confirmed in large phase III trials (1, 11).

Extreme hypofractionation, using SBRT doses per fraction of $\geq$7.0 Gy, has many potential advantages, including improved clinical outcomes and fewer visits, improving patient convenience and departmental capacity. Prospective phase II studies of SBRT have focused on low- and intermediate-risk patients but have reported favorable biochemical outcomes for all risk groups (12, 13). The phase III PACE trial is testing 5-fraction SBRT against standard fractionation to establish whether the abbreviated schedule is noninferior. In advance of the randomized evidence, SBRT in 5 fractions appears to have promising efficacy and side effect profile.

To enhance personalized treatment, the dose can be escalated to the dominant intraprostatic lesion, which is the most common site of local recurrence (14, 15). This has been tested in the FLAME (investigate the benefit of a focal

lesion ablative microboost in prostate cancer) trial (ClinicalTrials.gov identifier, NCT01168479) (16) and the hypo-FLAME (hypofractionated focal lesion ablative microboost in prostate cancer) study (ClinicalTrials.gov identifier, NCT02853110). The concept of "biological conformality" (17) uses the additional information from functional sequences to target the dose to the area most likely to benefit from dose escalation. In particular, diffusion weighted imaging (DWI) can be used to generate apparent diffusion coefficient maps to identify more aggressive disease, which might benefit from boosting (18-20).

The direction has been towards progressively more abbreviated RT schedules; thus, if 5-fraction SBRT is safe and effective, it raises the question of how low can we go (Fig. 1). Hoskin et al (21, 22) reported the longer term outcomes for mainly intermediate- and high-risk patients who underwent high-dose-rate brachytherapy (HDR-BT) alone. A dose of either 3 fractions at 10.5 Gy or 2 fractions at 13 Gy gave acceptable toxicity rates, with 91% to 93% free of biochemical relapse at 4 years (22). The same group reported early toxicity data showing single-fraction prostate HDR-BT with 19 Gy is tolerable, although a significant increase in the need for catheterization was seen compared with the 2-fraction cohort, in particular, when 20 Gy was delivered to the whole gland (23). However, late toxicity and biochemical control were similar for a single 19- to 20-Gy fraction compared with 2 to 3 fractions (22). Other groups have reported favorable toxicity rates with single-fraction HDR-BT (24, 25). Prada et al (24) reported low morbidity in patients treated with single-fraction 19-Gy HDR-BT monotherapy with injections of transperineal hyaluronic acid into the perirectal fat. However, no margin was added to the prostate for the planning target volume, and the biochemical control rate was 66% at 6 years. The urethral dose can be a limiting factor to the total dose achieved, as seen when HDR-BT is used to plan an intraprostatic boost (26).

Low-dose-rate brachytherapy is also an option for dose escalation, with low toxicity rates and excellent biochemical control (27, 28) and without the need for a shielded room such as required for HDR-BT. In the ASCENDE-RT (an analysis of survival endpoints for a randomized trial comparing a low-dose-rate brachytherapy boost to a dose-escalated external beam RT) trial, the use of low-dose-rate BT as a boost improved biochemical progression-free survival compared with dose-escalated external beam RT alone (29); however, this was at the cost of higher genitourinary toxicity (30). Although brachytherapy might be considered the ultimate in conformal treatment, it is invasive and requires patients to meet anatomic criteria and is therefore not broadly available to all patients. In contrast, linear accelerator (linac)-based single-fraction treatment would potentially be feasible across the globe. It might even offer cost-effective benefits compared with brachytherapy or multiple-fraction treatment and allow higher patient throughput on a single machine.

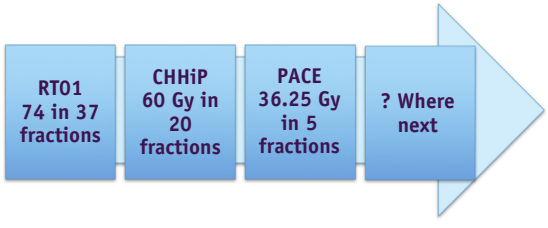

Fig. 1. Progression of radiation therapy trials within the United Kingdom during the past 15 years. *Abbreviations:* CHHiP = conventional or hypofractionated high dose intensity modulated radiotherapy for prostate cancer; PACE = prostate advances in comparative evidence; RT01 = Medical Research Council RT01.

It is technically feasible to deliver similar target doses and meet the same constraints of HDR-BT using external beam RT (31). SBRT can be used to deliver an equivalent biologically effective dose without the need for a surgical procedure, general anesthesia, and associated potential complications. This is being assessed within the phase II PROSINT (phase II study of ultra-high-dose hypofractionated vs single-dose image-guided radiotherapy for prostate cancer) trial (ClinicalTrials.gov identifier, NCT02570919) randomizing between 45 Gy in 5 fractions and a single 24-Gy fraction.

Given the higher dose per fraction, highly conformal dose distribution, and steep dose gradient seen with SBRT, accurate delivery using direct tumor motion monitoring and online adaptive RT (ART) methods has become even more important. The ideal delivery system would consist of optimal image guidance (before treatment and intrafraction MRI), rapid delivery, and intrafraction ART.

Future of Image-Guided RT

MRgRT Platforms

MRgRT systems provide what has long been considered the "holy grail" of RT delivery, the integration of an MRI scanner that can provide clinical quality imaging with a modern linear accelerator (32). Several systems are in development for clinical use (33-36); these have been summarized in Table 1. Not only can the improved soft tissue contrast of MRI improve patient positioning before RT "on-line," but "real-time" imaging during treatment delivery itself can also help to detect the tumor and normal tissue position and deliver the radiation dose more precisely.

The MRIdian system (ViewRay Inc, Oakwood Village, OH), with integrated options of either tricobalt-60 or, more recently, a 6-megavoltage linac, has been treating patients since 2014, and the first patient was treated using the Elekta MR-Linac (Elekta AB, Stockholm, Sweden) in May 2017. Despite the potential effect on dose distribution by the magnetic field (37), which increases with higher field strength (38), treatment plan quality equivalency to standard linacs is

Table 1 Magnetic resonance imaging-guided radiation platforms existing or in development

Variable	Type of system	Magnetic field orientation	Research/ clinical status	Adaptive capabilities
Elekta MR-Linac (29)	1.5-T, 7-MV; 70-cm closed bore; single-focused Agility MLC providing 5-mm resolution for nominal 100-cm SSD, projecting to 7 mm at the isocenter	B_0 magnetic field perpendicular to delivery	First patient treated May 2017 in Utrecht as part of First In Man protocol	ART capabilities include 1. Shifting plan to overlay anatomy—simple dose shift 2. Offline ART 3. Library of plans 4. Online ART—segment-weight optimization and full reoptimization available 5. Visual tracking of target
ViewRay MRIdian cobalt-60 system (30)	0.35-T Cobalt system, 3 ^{60}Co heads on rotating gantry ring; split magnet 70-cm closed bore	B_0 magnetic field perpendicular to delivery	FDA 510(k) cleared for cobalt systems; treated patients since 2014 on cobalt system	ART capabilities include 1. Shifting plan to overlay anatomy—couch shift 2. Offline ART 3. Library of plans 4. Online ART—segment-weight optimization and full reoptimization available 5. Tracking with exception gating for target
ViewRay MRIdian Linac system	Newer system with 6-MV linac, split magnet 70-cm bore "Razor" MLC is a double-stacked, double-focused MLC, 8-mm leaf width, providing 4-mm resolution and allowing field sizes down to 2 × 4 mm	B_0 magnetic field perpendicular to delivery	FDA 510(k) cleared for linac system; treated patients since 2017 on linac system	ART capabilities include 1. Shifting plan to overlay anatomy—couch shift 2. Offline ART 3. Library of plans 4. Online ART—segment-weight optimization and full reoptimization available 5. Tracking with exception gating for target
Sydney Inline Australian MRI-LINAC system (31)	1.0 T 6-MV 82-cm open bore	B_0 magnetic field perpendicular and parallel to delivery	Currently, a research system	NA
MagnetTx Aurora RT Linac-MR (32)	0.5 T, 6-MV	B_0 magnetic field parallel to delivery	Currently, a research system	NA

Abbreviations: ART = adaptive radiation therapy; FDA = Food and Drug Administration; linac = linear accelerator; MR = magnetic resonance; MRI = magnetic resonance imaging; MV = megavoltage; NA = not available; SSD = solid-state drive.

achievable (39, 40). The dosimetric effect of the Lorentz force can be accounted for and mitigated through Monte Carlo dose calculations and inverse planning techniques.

Benefits and Challenges of MRI

MRI in RT planning provides superior soft tissue differentiation with the added capability of functional imaging. Improved image contrast has also been demonstrated with MRgRT systems, with which even low field strength from an on-board 0.35 T MRI can give improved anatomic visualization compared with on-board CT (41), with a reduction in radiation exposure. Figure 2 shows clinical true fast imaging with steady-state precision MR sequence from ViewRay MRIdian system of the prostate.

MRI sequences could also be used as an indicator of tumour response. Some preliminary results of DWI with MRgRT have been reported (42), although, currently, no validated MRI biomarkers are available for prostate RT. MR images acquired throughout a course of MRgRT could allow the dose distribution to be adjusted based on the tumor response. Adaptive dose painting can target the index lesion, where local relapse is most likely to occur (14, 20), or areas of more aggressive disease (18, 19). Currently, a paucity of data assessing imaging changes during and directly after treatment is available; however, studies have shown that the apparent diffusion coefficient values from DWI increase after treatment (43-45), with the greatest changes seen in patients with better outcomes (44).

The integration of MRI into the different stages of RT from target identification to planning to delivery is clearly attractive. However, limitations exist, including the limited availability of MRI scanners, medical contraindications to MRI, and the relatively reduced familiarity with MRI by radiation oncologists compared with CT. In addition, MRI introduces technical hurdles within the planning process, including the lack of direct electron density information, organ motion between the CT and MRI scans, and geometric distortion. Conventional immobilization with MR receiver coils presents additional challenges. Obstacles also include culture changes when a radiation oncology department houses an MRI scanner. Although integration of MR simulators is becoming more commonplace in radiation oncology departments, the need to incorporate MRI safety poses unique challenges.

Daily Adaptive Replanning

Benefits of Daily Adaptive Replanning

With standard IGRT, no method is available to compensate for the independent movements of the 4 potential RT targets—prostate, seminal vesicles, pelvic lymph nodes, and intraprostatic boost. RT can induce an initial increase in the size of the prostate, followed by constriction at the end of RT (46, 47). With SBRT, the swelling can persist even after the end of treatment (48).

Despite daily IGRT to compensate for interfraction movement, residual deformation of the prostate and the organs at risk (OAR) (47, 49) with ongoing intrafraction motion of the prostate continues to be a challenge (50). Offline adaptation can adjust for systematic changes; however, Peng et al (51) showed that when the original treatment plan is superimposed on daily in-room CT scans, approximately one-third of the fractions would need online replanning owing to the discrepancy in the planned and delivered dose.

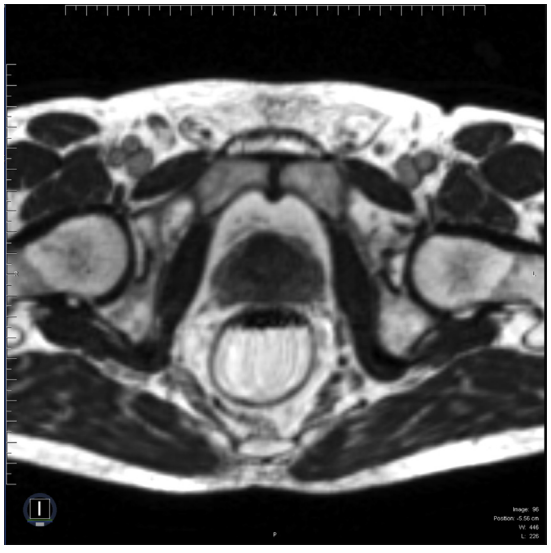

Fig. 2. A clinical true fast imaging with steady-state precision magnetic resonance sequence from ViewRay MRIdian system with acquisition in 25 seconds.

The implications of this disparity become more significant with a shorter ultrafractionated treatment course. On-table, online ART is now feasible with MRgRT and represents an attractive solution for ultrahypofractionated prostate RT. Online ART has the ability to account for not only systematic anatomic changes of prostate swelling, but also random anatomic changes, such as inter- and intrafraction bladder and rectal filling, in addition to independent movement and deformation of multiple targets.

Daily Adaptive Replanning—Obstacles and Solutions

The solution for optimal delivery of a planned dose is real-time planning and daily online adaptation. A number of steps are involved in using the newly acquired images to adjust for changes in anatomy (Fig. 3).

We have defined 6 strategies for ART:

1. Shifting the plan to overlay anatomy: The dose is adapted by shifting the plan relative to the anatomy (3-dimensional or 6-dimensional correction) or vice versa. This is equivalent to standard IGRT.
2. Dynamic shifting of a plan with tracking: This requires intrafraction motion monitoring and has been shown to be feasible with prostate cancer with Calypso beacons (52).
3. Offline ART: This is correct for systematic deformations of the targets (53) or OARs that occur slowly during the RT course, plus shifting the plan on the day of treatment as in strategy 2.
4. Library of plans: Selection is from plans for varying patient anatomy and to deliver the best fit for the anatomy of the day (54, 55).
5. Online ART: This is used to adapt the plan on a daily basis after imaging and to re-optimize or create a new treatment plan.
6. Real-time (intrafraction) ART: This is used to adapt the planned dose during an RT fraction.

The strategies most relevant to prostate MRgRT (strategies 1, 5, and 6) are discussed in the subsequent sections and summarized in Figure 4. The offline strategies 3 and 4 can be performed in lieu of strategy 5, when departmental resources limit the ability to perform on-table ART. All 6 strategies can be used with MRgRT gating in the presence of accurate beam-on imaging.

Shifting the Plan to Overlay Anatomy

IGRT repositioning

Online approaches (56) adjust for interfraction displacements of 1 selected RT target using a couch shift technique and keeping the treatment plan the same.

Simple dose shift

The pretreatment dose distribution itself is translated and rotated according to the change in anatomy (57). This

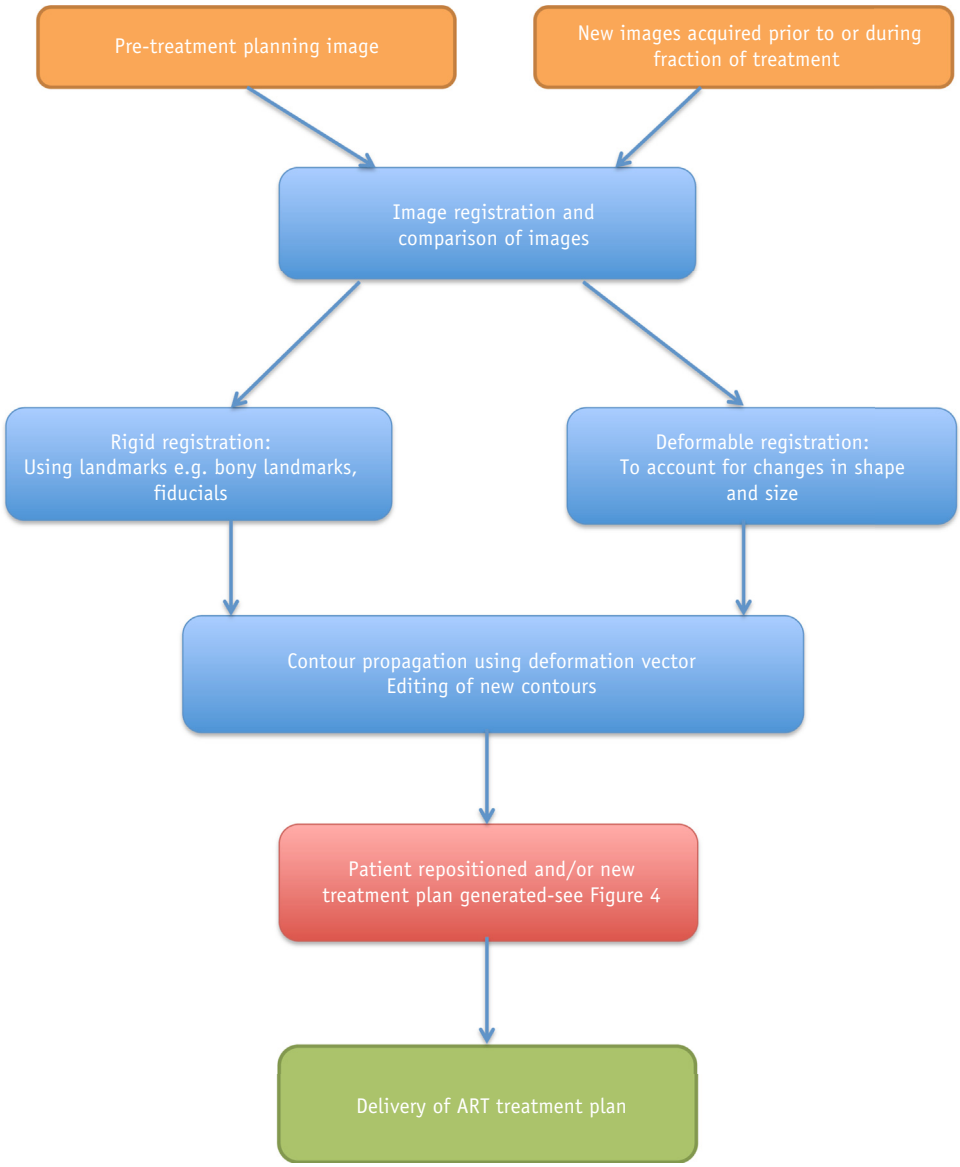

Fig. 3. Flow chart summarizing the steps in adaptive radiation therapy (ART).

method does not require full reoptimization of a plan and is therefore a rapid IGRT solution. A similar method has been described for online rotational correction by adjusting the gantry and collimator angles (58).

Real-time imaging with gated delivery

The challenge of intrafraction motion can be mitigated using gating strategies, whereby tumor motion monitoring is used in conjunction with visual inspection or an automated algorithm to adjust treatment delivery. "Exception gating" uses a specified threshold, eg, with a 2-mm/5-s threshold, if the movement of the prostate exceeds 2 mm from baseline for >5 seconds, treatment delivery is paused to allow for a return of the prostate to the initial position, adaptation of patient position, or a simple dose shift.

At present, prostate motion can be monitored using x-ray tracking of implanted radiopaque markers (seeds) (59, 60) or the Calypso system using electromagnetic transponders (52). MRgRT using soft tissue matching, however, does not require the implantation of seeds or additional radiation exposure and allows visualization of target and normal tissue motion and deformation. The accuracy of target localization is dependent on the speed of image acquisition. Gating through MRI in a clinical setting has been demonstrated with the MRIdian system, where motion monitoring is performed on a sagittal plane acquired at 4 frames per second, followed by real-time deformation and segmentation of the region of interest (61). However, this would be further improved using 3D imaging and patient individualization of the threshold margin, which might include motion prediction algorithms (62).

Online adaptive replanning

A number of methods with various levels of complexity are available for adaptive replanning. Most studies to date have

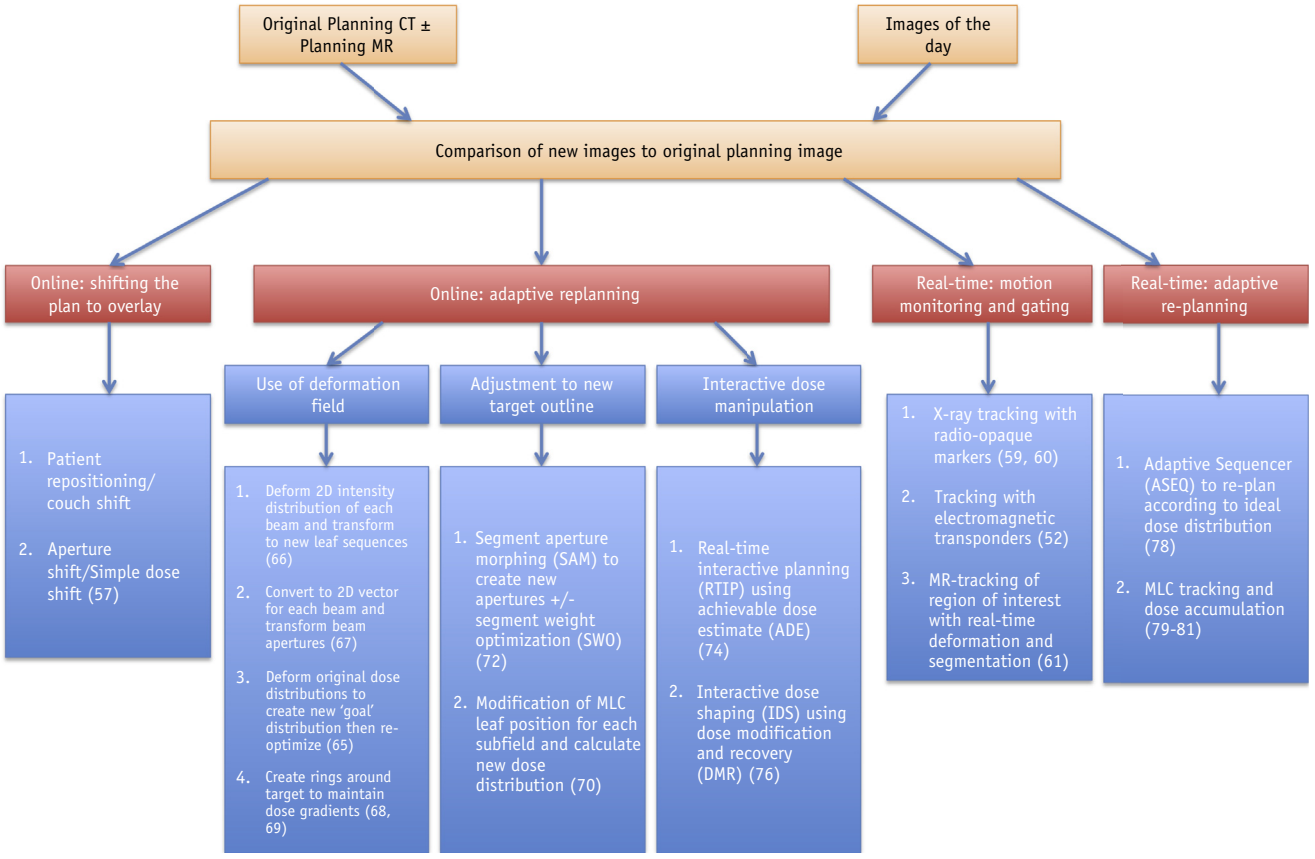

Fig. 4. Flow chart summarizing the spectrum of adaptive radiation therapy (ART). *Abbreviations:* CT = computed tomography; MLC = multileaf collimator; MR = magnetic resonance.

used cone beam CT for daily imaging, which provides a poorer image quality (compared with planning CT and MRI) for new contours, followed by plan adaptation.

The "Blue Sky" aim would be eventually to dispense with pretreatment planning completely and create an online plan from the beginning each day to reflect the current anatomy. This can be in tandem with dose painting based on the distribution of the tumor load as described previously (63). Online MRgRT has been demonstrated clinically with daily MRI by reoptimizing using the original beam angles and objectives used if the constraints were not met (64). Just greater than one-half of the fractions were treated using an adapted plan. The median time for ART was 26 minutes and was well tolerated.

Because this process needs to be completed in a timely manner, several approaches have described adjusting the initial plan, without full optimization, for expediency. Rapid replanning is especially important because increased organ motion over time could negate any benefit from ART.

Use of the deformation field

The deformation matrix created by registering the daily verification images to the planning images can be used to alter the original plan accordingly. Comparison of the whole target or points on the target (65) in the beam's eye view can be used to modify each segment (66) or beam aperture (67). Alternatively, the method of gradient maintenance (68) creates a series of partial concentric rings around the target with the aim of retaining the dose gradients toward each OAR. A similar method has been described with the MRIdian system, whereby rings control the gradients and autosegmentation through deformation, to minimize the recontouring required (69).

Adjustment to new target outline

To avoid the complexities of deformable image registration (DIR), methods to simply compare the target outline are available (70, 71). Segment aperture morphing can adjust the segment shapes to the new target contour (72), with a further step of segment weight optimization for larger deformations. Online replanning methods that are suitable for implementation with the Elekta MR-Linac have also been reported (71, 73).

Interactive dose manipulation

This approach enables the clinician to use tools to click on or select a part of the plan and "drag" the isodose curves or

dose-volume histogram and view the updated dose distribution (74-76). Constraints can be defined that should not be violated, to preserve, for example, a minimum dose to the target (74). In the future, these could allow for real-time automated modification of a plan to the anatomy of the day both before and during treatment.

Real-time adaptive replanning

The methods described so far have mainly focused on the target outline alone, and although they can improve target coverage compared with patient repositioning alone (66, 67, 70), ultimately replanning from the beginning will yield the best dosimetry. Real-time ART can improve dose accuracy, regardless of the delivery system (77). The only way this can be achieved is by continuous imaging with constant replanning, including reoptimization. Treatment planning systems are already capable of rapid dose calculations using cloud computing.

The ultimate goal of adaptive replanning will be to adapt a plan during beam delivery. Kontaxis et al (78) have described a graphics-processing unit, Monte Carlo dose engine, inverse dose optimization algorithm, and an adaptive sequencer to calculate deliverable intensity modulated RT plans. New images are fed into this system in real time. Starting with an ideal dose, the sequencer calculates each segment and the dose that it will deliver, subtracting this from the initially calculated "ideal" dose distribution. This step is repeated with multiple iterations to achieve the ideal dose. Treatment can start before the final dose calculation is complete, allowing the constantly changing anatomy to affect the optimization and preventing a delay in treatment. At the end of each fraction, the actual dose delivered is used to calculate any excess in dose or shortfall, which is then compensated for by adjusting the dose calculations in the subsequent fractions.

Real-time multileaf collimator tracking has been demonstrated to improve dose delivery in a clinical setting for prostate patients using the Calypso localization system (79). If accurate online dose reconstruction is available, this can provide a rapid calculation of the dose delivered so far within a fraction to adjust the dose for the remaining fraction delivery time and allow intrafraction replanning. This has been described for dynamic multileaf collimator tracking (80) and can be used to reoptimize a plan in the time taken for the gantry to rotate between beams for uninterrupted treatment (81).

Although such solutions are attractive, they assume that DIR is a well-solved problem. However, the bladder, rectum, and prostate deform in a nonuniform manner. This makes the quality assurance of accurately documenting the delivered dose challenging, and novel methods of time-efficient quality assurance are required (82).

Before adaptive intrafraction replanning becomes a reality, efforts are currently focused on expediting imaging, replanning and beam-on times such that intrafraction adaptation is not required.

Autosegmentation

Benefits of autosegmentation

Having a clinician recontour a patient in real time as a part of an adaptive workflow is not feasible on a daily basis. The advantages of autosegmentation are a reduction in the time required for delineation and decreased interobserver variability (83, 84). For real-time ART, autosegmentation will allow rapid replanning using real-time images, ultimately without the need for a clinician to be present.

Obstacles to autosegmentation and solutions

Multiple methods are available for autosegmentation, with the most basic techniques using features of imaging alone such as grayscale measures to create contours. However, the more sophisticated, rapidly evolving automated atlas-based segmentation software uses a pre-existing library of contoured reference atlases to automatically generate contours on a new set of images using rigid image registration or DIR. Multiple-atlas methods such as simultaneous truth and performance level estimation (85) and majority vote create autocontours from a number of fused atlases and are therefore more accurate than single-atlas methods. Greater weighting can be given to the atlases chosen by the software to have anatomy most similar to the plan in question. The optimal number of atlases required will vary depending on the software used and the structure to be delineated. Although additional atlases provide more comprehensive anatomic data, this is with the computational cost of additional time and the accuracy of the autocontour plateau with increasing atlas numbers (86).

The level of agreement between manually drawn contours and autocontours is dependent on the target volume. For prostate RT planning, good concordance has been seen for structures such as the femoral heads and bladder (86-88) and poor concordance for seminal vesicles and the penile bulb. Variable results have been seen for accuracy of prostate definition with CT; however, as expected, this improves when MRI is used for autodelineation (89, 90). MRI optimization, such as sequences improving the visualization of the prostate capsule, might further improve autocontouring (Fig. 5; PACE trial MRI sequence).

Although potential exists for these programs to improve efficiency, the current limitation result from the huge variability in pelvic anatomy and the poor soft tissue contrast previously seen with various CT modalities (91, 92). In the first case, review and editing of any autocontours are required (93, 94).

Segmentation for target tracking must be both rapid and accurate but will depend on image contrast, MR field strength, and the method of autosegmentation used (95). For atlas-based methods with real-time intrafraction segmentation, the reference atlas is patient-specific and DIR

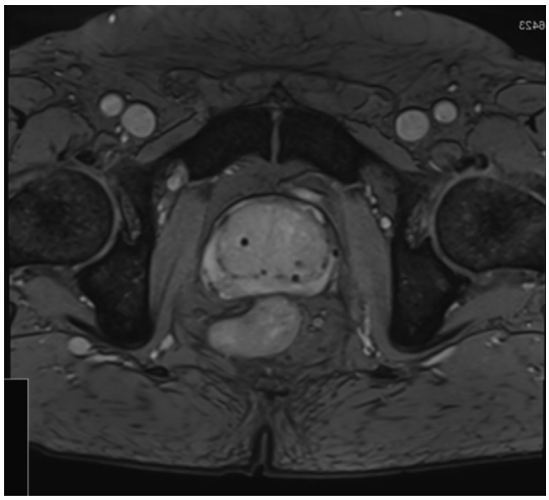

Fig. 5. Magnetic resonance image using adaptation of the "medic" T2-weighted Siemens sequence showing prostate capsule and fiducial markers (image courtesy of Maria Schmidt, Institute of Cancer Research).

and the resultant "intrapatient" autocontours are more accurate (84, 96, 97) and time efficient.

MRI-Only Workflow

Benefits of MRI-only workflow

RT planning currently uses CT imaging, which provides the relevant electron density required for dose calculations. A mixed CT-MRI workflow requires image coregistration, which incurs the risk of introducing inaccuracy as a result of discrepancies in patient positioning, imaging information, and anatomic changes between scans. The latter is particularly relevant for prostate cancer patients, in whom bladder and rectal filling can vary between scans, although minimizing the time between CT and MRI acquisitions can reduce this problem.

The registration error has been estimated to be approximately 2 mm (98) and remains a problem even when using gold fiducial markers to coregister the CT and MRI scans (99), although the "real truth" of image registration inaccuracy is unknown. However, the ultimate goal of the MRgRT system would be to avoid the need for fiducial markers, which require extra resources for insertion and have associated risks for the patients.

Planning directly on an MRI scan removes the systematic error of coregistration (100), which might be large enough to counteract any advantage from the addition of MRI into the process. MRI-only workflow requires a synthetic CT or pseudo-CT scan (101, 102) to give the electron density information required for dose calculations. A major challenge when using MRI is geometric distortion, which can result from either machine-related or patient-related factors. Geometric distortion is greater at a distance from the center of the field; however, for accurate dose calculation, the spatial integrity maintained to the skin surface is essential. This should be minimized using postprocessing before the use of images for planning (102). Efforts have been made to characterize correction maps; however, further work is needed to quantify and develop methods for mitigating geometric distortion (103).

Obstacles to MRI-only workflow and solutions

A number of methods are available to create a pseudo- or synthetic CT scan. These include tissue segmentation, atlas mapping method, and voxel method.

Tissue segmentation

After manual or automatic segmentation of an MRI data set, assigning separate densities to air, soft tissue, and bone is more accurate than applying a single electron density equivalent to water to the whole body (104, 105) and gives comparable results to the standard method of a planning CT scan (105, 106). However, bone segmentation is time consuming using standard MRI sequences, and the value used for the assigned densities must also be relevant (105, 107, 108).

Atlas mapping method

The first step for the atlas mapping method (109, 110) involves the generation of MRI and pseudo-CT atlases from patient data. When MRI data from a new patient is acquired, the same deformations required to register the compiled MRI atlas to the new MR images are applied to the pseudo-CT atlas to map the electron density information to the new patient. A comparison of the standard planning CT scan to the pseudo-CT scan gave a dose difference of $<2\%$ (109, 111), in agreement with data from other MRI planning studies (104, 112). This method can also be used to propagate contours (109, 110); however, it does have limitations, with atypical patient anatomy and the initial step of atlas formation requiring DIR, with the potential errors as described in previous sections.

Voxel method

Statistical models to differentiate the attenuation of tissue types have been investigated to allow the automatic conversion of the MRI intensity in each voxel to a Hounsfield unit (113-115). Using the information from all voxels, a greater spectrum of attenuation coefficients is obtained for a more accurate dose calculation, rather than the limited number used with tissue segmentation (115, 116).

Ultimately, an automated approach for pseudo-CT generation, combining the described methods, will be more clinically useful. The now commercially available Philips MRCAT (MR for calculation attenuation) creates a pseudo-CT scan from an mDIXON sequence, acquired with 2 echo times. The initial step comprises model-based automatic tissue segmentation into the 5 classes of air, fat, water-rich tissue, spongy bone, and compact bone. In the second step,

each voxel is assigned a pseudo-Hounsfield unit value based on density values. A number of factors contribute to dose calculations in this process (117); however, the workflow appears to be dosimetrically accurate compared with CT-based planning (118) and has been implemented clinically in prostate RT (119).

MRI-only workflow is now a realistic prospect in the near future and could improve the accuracy of RT planning.

Conclusions

The technological revolution in RT planning now allows us to ask questions, which a decade ago would have been impossible to answer. The increased precision in every step might allow us to further hypofractionate prostate cancer RT, perhaps even down to a single fraction, such as has been demonstrated with brachytherapy. Although this could be delivered using CT guidance, the ideal technology would be MRgRT. Intrafraction MRI, automatic contouring, and fast online and real-time adaptive replanning allow us to challenge the accepted dogma of the RT planning workflow.

To achieve this vision, many hurdles lie ahead, and high quality clinical research is necessary. The challenges are clear and the benefit is yet to be realized. As a wise man once said, "a journey of a thousand miles starts with a single step."

References

1. Dearnaley D, Syndikus I, Mossop H, et al. Conventional versus hypofractionated high-dose intensity-modulated radiotherapy for prostate cancer: 5-Year outcomes of the randomised, non-inferiority, phase 3 CHHiP trial. *Lancet Oncol* 2016;17:1047-1060.
2. Dasu A, Toma-Dasu I. Prostate alpha/beta revisited—an analysis of clinical results from 14 168 patients. *Acta Oncol* 2012;51:963-974.
3. Brenner DJ, Martinez AA, Edmundson GK, et al. Direct evidence that prostate tumors show high sensitivity to fractionation (low α/β ratio), similar to late-responding normal tissue. *Int J Radiat Oncol Biol Phys* 2002;52:6-13.
4. Tree AC, Alexander EJ, Van As NJ, et al. Biological dose escalation and hypofractionation: What is there to be gained and how will it best be done? *Clin Oncol* 2013;25:483-498.
5. Tree AC, Khoo VS, van As NJ, et al. Is biochemical relapse-free survival after profoundly hypofractionated radiotherapy consistent with current radiobiological models? *Clin Oncol (R Coll Radiol)* 2014;26:216-229.
6. Dearnaley DP, Jovic G, Syndikus I, et al. Escalated-dose versus control-dose conformal radiotherapy for prostate cancer: Long-term results from the MRC RT01 randomised controlled trial. *Lancet Oncol* 2014;15:464-473.
7. Viani GA, Stefano EJ, Afonso SL. Higher-than-conventional radiation doses in localized prostate cancer treatment: A meta-analysis of randomized, controlled trials. *Int J Radiat Oncol Biol Phys* 2009;74:1405-1418.
8. Zietman AL, DeSilvio ML, Slater JD, et al. Comparison of conventional-dose vs high-dose conformal radiation therapy in clinically localized adenocarcinoma of the prostate: A randomized controlled trial. *JAMA* 2005;294:1233-1239.
9. Fowler J, Chappell R, Ritter M. Is α/β for prostate tumors really low? *Int J Radiat Oncol Biol Phys* 2001;50:1021-1031.
10. Miralbell R, Roberts SA, Zubizarreta E, et al. Dose-fractionation sensitivity of prostate cancer deduced from radiotherapy outcomes of 5,969 patients in seven international institutional datasets: $\alpha/\beta = 1.4$ (0.9-2.2) Gy. *Int J Radiat Oncol Biol Phys* 2012;82:e17-e24.
11. Incrocci L, Wortel RC, Alemayehu WG, et al. Hypofractionated versus conventionally fractionated radiotherapy for patients with localised prostate cancer (HYPRO): Final efficacy results from a randomised, multicentre, open-label, phase 3 trial. *Lancet Oncol* 2016;17:1061-1069.
12. Loblaw A, Cheung P, D'Alimonte L, et al. Prostate stereotactic ablative body radiotherapy using a standard linear accelerator: Toxicity, biochemical, and pathological outcomes. *Radiother Oncol* 2013;107:153-158.
13. King CR, Brooks JD, Gill H, et al. Long-term outcomes from a prospective trial of stereotactic body radiotherapy for low-risk prostate cancer. *Int J Radiat Oncol Biol Phys* 2012;82:877-882.
14. Cellini N, Morganti AG, Mattiucci GC, et al. Analysis of intraprostatic failures in patients treated with hormonal therapy and radiotherapy: Implications for conformal therapy planning. *Int J Radiat Oncol Biol Phys* 2002;53:595-599.
15. Arrayeh E, Westphalen AC, Kurhanewicz J, et al. Does local recurrence of prostate cancer after radiation therapy occur at the site of primary tumor? Results of a longitudinal MRI and MRSI study. *Int J Radiat Oncol Biol Phys* 2012;82:e787-e793.
16. Lips IM, van der Heide UA, Haustermans K, et al. Single blind randomized phase III trial to investigate the benefit of a focal lesion ablative microboost in prostate cancer (FLAME-trial): Study protocol for a randomized controlled trial. *Trials* 2011;12:255.
17. Ling CC, Humm J, Larson S, et al. Towards multidimensional radiotherapy (MD-CRT): Biological imaging and biological conformality. *Int J Radiat Oncol Biol Phys* 2000;47:551-560.
18. deSouza NM, Riches SF, Van As NJ, et al. Diffusion-weighted magnetic resonance imaging: A potential non-invasive marker of tumour aggressiveness in localized prostate cancer. *Clin Radiol* 2008;63:774-782.
19. van As NJ, de Souza NM, Riches SF, et al. A study of diffusion-weighted magnetic resonance imaging in men with untreated localised prostate cancer on active surveillance. *Eur Urol* 2009;56:981-988.
20. Pathmanathan AU, Alexander EJ, Huddart RA, et al. The delineation of intraprostatic boost regions for radiotherapy using multimodality imaging. *Future Oncol* 2016;12:2495-2511.
21. Hoskin P, Rojas A, Ostler P, et al. High-dose-rate brachytherapy with two or three fractions as monotherapy in the treatment of locally advanced prostate cancer. *Radiother Oncol* 2014;112:63-67.
22. Hoskin P, Rojas A, Ostler P, et al. Single-dose high-dose-rate brachytherapy compared to two and three fractions for locally advanced prostate cancer. *Radiother Oncol* 2017;124:56-60.
23. Hoskin P, Rojas A, Ostler P, et al. High-dose-rate brachytherapy alone given as two or one fraction to patients for locally advanced prostate cancer: Acute toxicity. *Radiother Oncol* 2014;110:268-271.
24. Prada PJ, Jimenez I, González-Suárez H, et al. High-dose-rate interstitial brachytherapy as monotherapy in one fraction and transperineal hyaluronic acid injection into the perirectal fat for the treatment of favorable stage prostate cancer: Treatment description and preliminary results. *Brachytherapy* 2012;11:105-110.
25. Krauss DJ, Ye H, Martinez AA, et al. Favorable preliminary outcomes for men with low- and intermediate-risk prostate cancer treated with 19-Gy single-fraction high-dose-rate brachytherapy. *Int J Radiat Oncol Biol Phys* 2017;97:98-106.
26. Dankulchai P, Alonzi R, Lowe GJ, et al. Optimal source distribution for focal boosts using high dose rate (HDR) brachytherapy alone in prostate cancer. *Radiother Oncol* 2014;113:121-125.
27. Morris WJ, Keyes M, Spadinger I, et al. Population-based 10-year oncologic outcomes after low-dose-rate brachytherapy for low-risk and intermediate-risk prostate cancer. *Cancer* 2013;119:1537-1546.

28. Zaorsky NG, Davis BJ, Nguyen PL, et al. The evolution of brachytherapy for prostate cancer. *Nat Rev Urol* 2017;14:415-439.
29. Morris WJ, Tyldesley S, Rodda S, et al. Androgen suppression combined with elective nodal and dose escalated radiation therapy (the ASCENDE-RT trial): An analysis of survival endpoints for a randomized trial comparing a low-dose-rate brachytherapy boost to a dose-escalated external beam boost for high- and intermediate-risk prostate cancer. *Int J Radiat Oncol Biol Phys* 2017;98:275-285.
30. Rodda S, Tyldesley S, Morris WJ, et al. ASCENDE-RT: An analysis of treatment-related morbidity for a randomized trial comparing a low-dose-rate brachytherapy boost with a dose-escalated external beam boost for high- and intermediate-risk prostate cancer. *Int J Radiat Oncol Biol Phys* 2017;98:286-295.
31. Henderson D, Tree A, van As N. Single fraction external beam radiotherapy for localised prostate cancer: A planning study. *Clin Oncol* 2017;29:e87.
32. Choudhury A, Budgell G, MacKay R, et al. The future of image-guided radiotherapy. *Clin Oncol* 2017;29:662-666.
33. Raaymakers BW, Lagendijk JJW, Overweg J, et al. Integrating a 1.5 T MRI scanner with a 6 MV accelerator: Proof of concept. *Phys Med Biol* 2009;54:N229.
34. Mutic S, Dempsey JF. The ViewRay System: Magnetic resonance-guided and controlled radiotherapy. *Semin Radiat Oncol* 2014;24:196-199.
35. Keall PJ, Barton M, Crozier S. The Australian magnetic resonance imaging-linac program. *Semin Radiat Oncol* 2014;24:203-206.
36. Fallone BG, Murray B, Rathee S, et al. First MR images obtained during megavoltage photon irradiation from a prototype integrated linac-MR system. *Med Phys* 2009;36(6 Pt 1):2084-2088.
37. Raaijmakers AJE, Raaymakers BW, van der Meer S, et al. Integrating a MRI scanner with a 6 MV radiotherapy accelerator: Impact of the surface orientation on the entrance and exit dose due to the transverse magnetic field. *Phys Med Biol* 2007;52:929-939.
38. Raaijmakers AJE, Raaymakers BW, Lagendijk JJW. Magnetic-field-induced dose effects in MR-guided radiotherapy systems: Dependence on the magnetic field strength. *Phys Med Biol* 2008;53:909-923.
39. Wooten HO, Green O, Yang M, et al. Quality of intensity modulated radiation therapy treatment plans using a ^{60}Co magnetic resonance image guidance radiation therapy system. *Int J Radiat Oncol Biol Phys* 2015;92:771-778.
40. Pathmanathan A, Nill S, Oelfke U, et al. Stereotactic body radiotherapy (SBRT) for localised prostate cancer on the magnetic resonance linac. *Clin Oncol* 2017;29:141-204.
41. Noel CE, Parikh PJ, Spencer CR, et al. Comparison of onboard low-field magnetic resonance imaging versus onboard computed tomography for anatomy visualization in radiotherapy. *Acta Oncol* 2015;54:1474-1482.
42. Yang Y, Cao M, Sheng K, et al. Longitudinal diffusion MRI for treatment response assessment: Preliminary experience using an MRI-guided tri-cobalt 60 radiotherapy system. *Med Phys* 2016;43:1369-1373.
43. Park SY, Kim CK, Park BK, et al. Early changes in apparent diffusion coefficient from diffusion-weighted MR imaging during radiotherapy for prostate cancer. *Int J Radiat Oncol Biol Phys* 2012;83:749-755.
44. Liu L, Wu N, Ouyang H, et al. Diffusion-weighted MRI in early assessment of tumour response to radiotherapy in high-risk prostate cancer. *Br J Radiol* 2014;87:20140359.
45. Decker G, Mürtz P, Gieseke J, et al. Intensity-modulated radiotherapy of the prostate: Dynamic ADC monitoring by DWI at 3.0 T. *Radiother Oncol* 2014;113:115-120.
46. King BL, Butler WM, Merrick GS, et al. Electromagnetic transponders indicate prostate size increase followed by decrease during the course of external beam radiation therapy. *Int J Radiat Oncol Biol Phys* 2011;79:1350-1357.
47. Nichol AM, Brock KK, Lockwood GA, et al. A magnetic resonance imaging study of prostate deformation relative to implanted gold fiducial markers. *Int J Radiat Oncol Biol Phys* 2007;67:48-56.
48. Gunnlaugsson A, Kjellén E, Hagberg O, et al. Change in prostate volume during extreme hypo-fractionation analysed with MRI. *Radiat Oncol* 2014;9:1-6.
49. Kerkhof EM, van der Put RW, Raaymakers BW, et al. Variation in target and rectum dose due to prostate deformation: An assessment by repeated MR imaging and treatment planning. *Phys Med Biol* 2008;53:5623-5634.
50. McPartlin AJ, Li XA, Kershaw LE, et al. MRI-guided prostate adaptive radiotherapy—a systematic review. *Radiother Oncol* 2016;119:371-380.
51. Peng C, Ahunbay E, Chen G, et al. Characterizing interfraction variations and their dosimetric effects in prostate cancer radiotherapy. *Int J Radiat Oncol Biol Phys* 2011;79:909-914.
52. Kupelian P, Willoughby T, Mahadevan A, et al. Multi-institutional clinical experience with the Calypso system in localization and continuous, real-time monitoring of the prostate gland during external radiotherapy. *Int J Radiat Oncol Biol Phys* 2007;67:1088-1098.
53. Nijkamp J, Pos FJ, Nuver TT, et al. Adaptive radiotherapy for prostate cancer using kilovoltage cone-beam computed tomography: First clinical results. *Int J Radiat Oncol Biol Phys* 2008;70:75-82.
54. Chen W, Gemmel A, Rietzel E. A patient-specific planning target volume used in "plan of the day" adaptation for interfractional motion mitigation. *J Radiat Res* 2013;54(Suppl 1):i82-i90.
55. Xia P, Qi P, Hwang A, et al. Comparison of three strategies in management of independent movement of the prostate and pelvic lymph nodes. *Med Phys* 2010;37:5006-5013.
56. Létourneau D, Martinez AA, Lockman D, et al. Assessment of residual error for online cone-beam CT-guided treatment of prostate cancer patients. *Int J Radiat Oncol Biol Phys* 2005;62:1239-1246.
57. Bol GH, Lagendijk JJW, Raaymakers BW. Virtual couch shift (VCS): Accounting for patient translation and rotation by online IMRT re-optimization. *Phys Med Biol* 2013;58:2989-3000.
58. Rijkhorst E-J, Lakeman A, Nijkamp J, et al. Strategies for online organ motion correction for intensity-modulated radiotherapy of prostate cancer: Prostate, rectum, and bladder dose effects. *Int J Radiat Oncol Biol Phys* 2009;75:1254-1260.
59. Shimizu S, Nishioka K, Suzuki R, et al. Early results of urethral dose reduction and small safety margin in intensity-modulated radiation therapy (IMRT) for localized prostate cancer using a real-time tumor-tracking radiotherapy (RTRT) system. *Radiat Oncol* 2014;9:118.
60. Keall PJ, Ng JA, Juneja P, et al. Real-time 3D image guidance using a standard LINAC: Measured motion, accuracy, and precision of the first prospective clinical trial of kilovoltage intrafraction monitoring-guided gating for prostate cancer radiation therapy. *Int J Radiat Oncol Biol Phys* 2016;94:1015-1021.
61. Bohoudi O, Bruynzeel A, Senan S, et al. SP-0494: Using a MRI-guided radiation therapy system for prostate cancer patients. ESTRO 36. *Radiother Oncol* 2017;123(Suppl 1):S263.
62. Seregni M, Paganelli C, Lee D, et al. Motion prediction in MRI-guided radiotherapy based on interleaved orthogonal cine-MRI. *Phys Med Biol* 2016;61:872.
63. van Schie MA, Steenbergen P, Dinh CV, et al. Repeatability of dose painting by numbers treatment planning in prostate cancer radiotherapy based on multiparametric magnetic resonance imaging. *Phys Med Biol* 2017;62:5575-5588.
64. Acharya S, Fischer-Valuck BW, Kashani R, et al. Online magnetic resonance image guided adaptive radiation therapy: First clinical applications. *Int J Radiat Oncol Biol Phys* 2016;94:394-403.
65. Wu QJ, Danthai T, Zhiheng W, et al. On-line re-optimization of prostate IMRT plans for adaptive radiation therapy. *Phys Med Biol* 2008;53:673-691.
66. Mohan R, Zhang X, Wang H, et al. Use of deformed intensity distributions for on-line modification of image-guided IMRT to account for interfractional anatomic changes. *Int J Radiat Oncol Biol Phys* 2005;61:1258-1266.

67. Feng Y, Castro-Pareja C, Shekhar R, et al. Direct aperture deformation: An interfraction image guidance strategy. *Med Phys* 2006; 33:4490-4498.
68. Ahunbay EE, Li XA. Gradient maintenance: A new algorithm for fast online replanning. *Med Phys* 2015;42:2863-2876.
69. Bohoudi O, Bruynzeel AME, Senan S, et al. Fast and robust online adaptive planning in stereotactic MR-guided adaptive radiation therapy (SMART) for pancreatic cancer. *Radiother Oncol* 2017 [e-pub ahead of print]. http://dx.doi.org/10.1016/j.radonc.2017.07.028.
70. Fu W, Yang Y, Yue NJ, et al. A cone beam CT-guided online plan modification technique to correct interfractional anatomic changes for prostate cancer IMRT treatment. *Phys Med Biol* 2009;54:1691-1703.
71. Ahunbay EE, Ates O, Li XA. An online replanning method using warm start optimization and aperture morphing for flattening-filter-free beams. *Med Phys* 2016;43:4575-4584.
72. Ahunbay EE, Peng C, Chen G-P, et al. An on-line replanning scheme for interfractional variations. *Med Phys* 2008;35:3607-3615.
73. Ates O, Ahunbay EE, Moreau M, et al. Technical note: A fast online adaptive replanning method for VMAT using flattening filter free beams. *Med Phys* 2016;43:2756-2764.
74. Otto K. Real-time interactive treatment planning. *Phys Med Biol* 2014;59:4845-4859.
75. Kamerling CP, Ziegenhein P, Sterzing F, et al. Interactive dose shaping part 2: Proof of concept study for six prostate patients. *Phys Med Biol* 2016;61:2471-2484.
76. Ziegenhein P, Kamerling CP, Oelfke U. Interactive dose shaping part 1: A new paradigm for IMRT treatment planning. *Phys Med Biol* 2016;61:2457-2470.
77. Colvill E, Booth J, Nill S, et al. A dosimetric comparison of real-time adaptive and non-adaptive radiotherapy: A multi-institutional study encompassing robotic, gimbaled, multileaf collimator and couch tracking. *Radiother Oncol* 2016;119:159-165.
78. Kontaxis C, Bol GH, Lagendijk JJW, et al. Towards adaptive IMRT sequencing for the MR-linac. *Phys Med Biol* 2015;60:2493-2509.
79. Colvill E, Booth JT, O'Brien RT, et al. Multileaf collimator tracking improves dose delivery for prostate cancer radiation therapy: Results of the first clinical trial. *Int J Radiat Oncol Biol Phys* 2015;92:1141-1147.
80. Fast MF, Kamerling CP, Ziegenhein P, et al. Assessment of MLC tracking performance during hypofractionated prostate radiotherapy using real-time dose reconstruction. *Phys Med Biol* 2016;61:1546-1562.
81. Kamerling C, Fast M, Ziegenhein P, et al. TH-CD-202-12: Online inter-beam replanning based on real-time dose reconstruction. *Med Phys* 2016;43:3879.
82. Wang Y, Mazur TR, Park JC, et al. Development of a fast Monte Carlo dose calculation system for online adaptive radiation therapy quality assurance. *Phys Med Biol* 2017;62:4970-4990.
83. Tao C-J, Yi J-L, Chen N-Y, et al. Multi-subject atlas-based auto-segmentation reduces interobserver variation and improves dosimetric parameter consistency for organs at risk in nasopharyngeal carcinoma: A multi-institution clinical study. *Radiother Oncol* 2015; 115:407-411.
84. Hwee J, Louie AV, Gaede S, et al. Technology assessment of automated atlas based segmentation in prostate bed contouring. *Radiat Oncol* 2011;6:110.
85. Warfield SK, Zou KH, Wells WM. Simultaneous truth and performance level estimation (STAPLE): An algorithm for the validation of image segmentation. *IEEE Trans Med Imaging* 2004;23:903-921.
86. Wong WKH, Leung LHT, Kwong DLW. Evaluation and optimization of the parameters used in multiple-atlas-based segmentation of prostate cancers in radiation therapy. *Br J Radiol* 2016;89:20140732.
87. Velker VM, Rodrigues GB, Dinniwell R, et al. Creation of RTOG compliant patient CT-atlases for automated atlas based contouring of local regional breast and high-risk prostate cancers. *Radiat Oncol* 2013;8:188.
88. Greenham S, Dean J, Fu CKK, et al. Evaluation of atlas-based auto-segmentation software in prostate cancer patients. *J Med Radiat Sci* 2014;61:151-158.
89. Klein S, van der Heide UA, Lips IM, et al. Automatic segmentation of the prostate in 3D MR images by atlas matching using localized mutual information. *Med Phys* 2008;35:1407-1417.
90. Pasquier D, Lacornerie T, Vermandel M, et al. Automatic segmentation of pelvic structures from magnetic resonance images for prostate cancer radiotherapy. *Int J Radiat Oncol Biol Phys* 2007;68: 592-600.
91. Morrow NV, Lawton CA, Qi XS, et al. Impact of computed tomography image quality on image-guided radiation therapy based on soft tissue registration. *Int J Radiat Oncol Biol Phys* 2012;82:e733-e738.
92. Simmat I, Georg P, Georg D, et al. Assessment of accuracy and efficiency of atlas-based autosegmentation for prostate radiotherapy in a variety of clinical conditions. *Strahlenther Onkol* 2012;188:807-815.
93. Beasley WJ, McWilliam A, Slevin NJ, et al. An automated workflow for patient-specific quality control of contour propagation. *Phys Med Biol* 2016;61:8577-8586.
94. Altman MB, Kavanaugh JA, Wooten HO, et al. A framework for automated contour quality assurance in radiation therapy including adaptive techniques. *Phys Med Biol* 2015;60:5199-5209.
95. Feng Y, Kawrakow I, Olsen J, et al. A comparative study of automatic image segmentation algorithms for target tracking in MR-IGRT. *J Appl Clin Med Phys* 2016;17:441-460.
96. Li W, Vassil A, Zhong Y, et al. Daily dose monitoring with atlas-based auto-segmentation on diagnostic quality CT for prostate cancer. *Med Phys* 2013;40:111720.
97. Godley A, Sheplan Olsen LJ, Stephans K, et al. Combining prior day contours to improve automated prostate segmentation. *Med Phys* 2013;40:021722.
98. Roberson PL, McLaughlin PW, Narayana V, et al. Use and uncertainties of mutual information for computed tomography/magnetic resonance (CT/MR) registration post permanent implant of the prostate. *Med Phys* 2005;32:473-482.
99. Huisman HJ, Fütterer JJ, van Lin EN, et al. Prostate cancer: Precision of integrating functional MR imaging with radiation therapy treatment by using fiducial gold markers. *Radiology* 2005;236:311-317.
100. Nyholm T, Nyberg M, Karlsson MG, et al. Systematisation of spatial uncertainties for comparison between a MR and a CT-based radiotherapy workflow for prostate treatments. *Radiat Oncol* 2009; 4:54.
101. Nyholm T, Jonsson J. Counterpoint: Opportunities and challenges of a magnetic resonance imaging-only radiotherapy work flow. *Semin Radiat Oncol* 2014;24:175-180.
102. Schmidt AM, Payne SG. Radiotherapy planning using MRI. *Phys Med Biol* 2015;60:R323-R361.
103. Price RG, Kadbi M, Kim J, et al. Technical note: Characterization and correction of gradient nonlinearity induced distortion on a 1.0 T open bore MR-SIM. *Med Phys* 2015;42:5955-5960.
104. Chen L, Price RA Jr, Wang L, et al. MRI-based treatment planning for radiotherapy: Dosimetric verification for prostate IMRT. *Int J Radiat Oncol Biol Phys* 2004;60:636-647.
105. Jonsson JH, Karlsson MG, Karlsson M, et al. Treatment planning using MRI data: An analysis of the dose calculation accuracy for different treatment regions. *Radiat Oncol* 2010;5:62.
106. Korsholm ME, Waring LW, Edmund JM. A criterion for the reliable use of MRI-only radiotherapy. *Radiat Oncol* 2014;9:16.
107. Kim J, Garbarino K, Schultz L, et al. Dosimetric evaluation of synthetic CT relative to bulk density assignment-based magnetic resonance-only approaches for prostate radiotherapy. *Radiat Oncol* 2015;10:239.
108. Hu Y, Zhao W, Du D, et al. Magnetic resonance imaging-based treatment planning for prostate cancer: Use of population average

tissue densities within the irradiated volume to improve plan accuracy. *Pract Radiat Oncol* 2015;5:248-256.
109. Dowling JA, Lambert J, Parker J, et al. An atlas-based electron density mapping method for magnetic resonance imaging (MRI)-alone treatment planning and adaptive MRI-based prostate radiation therapy. *Int J Radiat Oncol Biol Phys* 2012;83:e5-e11.
110. Burgos N, Guerreiro F, McClelland J, et al. Iterative framework for the joint segmentation and CT synthesis of MR images: Application to MRI-only radiotherapy treatment planning. *Phys Med Biol* 2017;62:4237-4253.
111. Guerreiro F, Burgos N, Dunlop A, et al. Evaluation of a multi-atlas CT synthesis approach for MRI-only radiotherapy treatment planning. *Phys Med* 2017;35:7-17.
112. Uh J, Merchant TE, Li Y, et al. MRI-based treatment planning with pseudo CT generated through atlas registration. *Med Phys* 2014;41:051711.
113. Catana C, van der Kouwe A, Benner T, et al. Towards implementing an MR-based PET attenuation correction method for neurological studies on the MR-PET brain prototype. *J Nucl Med* 2010;51:1431-1438.
114. Berker Y, Franke J, Salomon A, et al. MRI-based attenuation correction for hybrid PET/MRI systems: A 4-class tissue segmentation technique using a combined ultrashort-echo-time/Dixon MRI sequence. *J Nucl Med* 2012;53:796-804.
115. Johansson A, Karlsson M, Nyholm T. CT substitute derived from MRI sequences with ultrashort echo time. *Med Phys* 2011;38:2708-2714.
116. Kapanen M, Tenhunen M. T1/T2*-weighted MRI provides clinically relevant pseudo-CT density data for the pelvic bones in MRI-only based radiotherapy treatment planning. *Acta Oncol* 2013;52:612-618.
117. Maspero M, Seevinck PR, Schubert G, et al. Quantification of confounding factors in MRI-based dose calculations as applied to prostate IMRT. *Phys Med Biol* 2017;62:948-965.
118. Tyagi N, Fontenla S, Zhang J, et al. Dosimetric and workflow evaluation of first commercial synthetic CT software for clinical use in pelvis. *Phys Med Biol* 2017;62:2961-2975.
119. Tyagi N, Fontenla S, Zelefsky M, et al. Clinical workflow for MR-only simulation and planning in prostate. *Radiat Oncol* 2017;12:119.